Supplementary Information for

Strongly coupled C@SiO_x/$MoSe_2$@NMWCNT heterostructure as anodes for Na^+ batteries with excellent stability and capacity

Mengru Bian,[a] Yincai Yang,[a] Youwen Chen,[a,*] Tiantian Wei,[a] Wei Deng,[a*] Biao Fu,[a] Renhua Qiu[a,*]

[a]College of Chemistry and Chemical Engineering, Hunan University, 410081,Changsha, China.

E-mail: renhuaqiu1@hnu.edu.cn, 36928664@qq.com

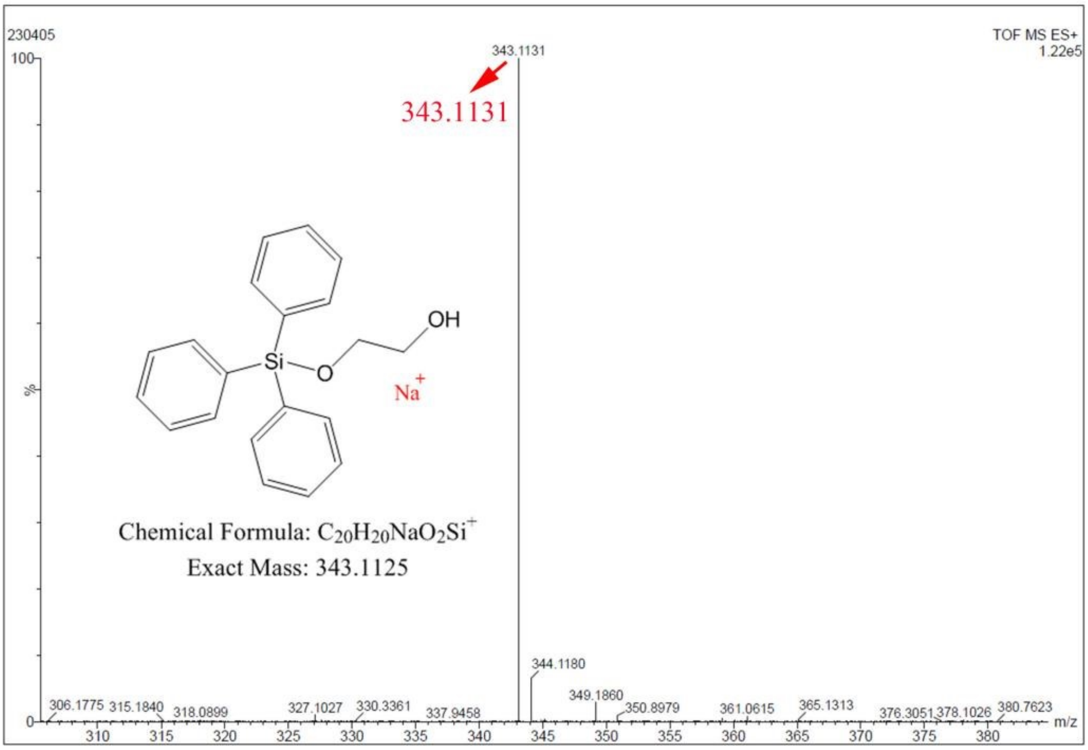

Fig. S1 Mass spectra of triphenyl silyl chloride ($(C_6H_5)_3SiCl$) mixed with EG.

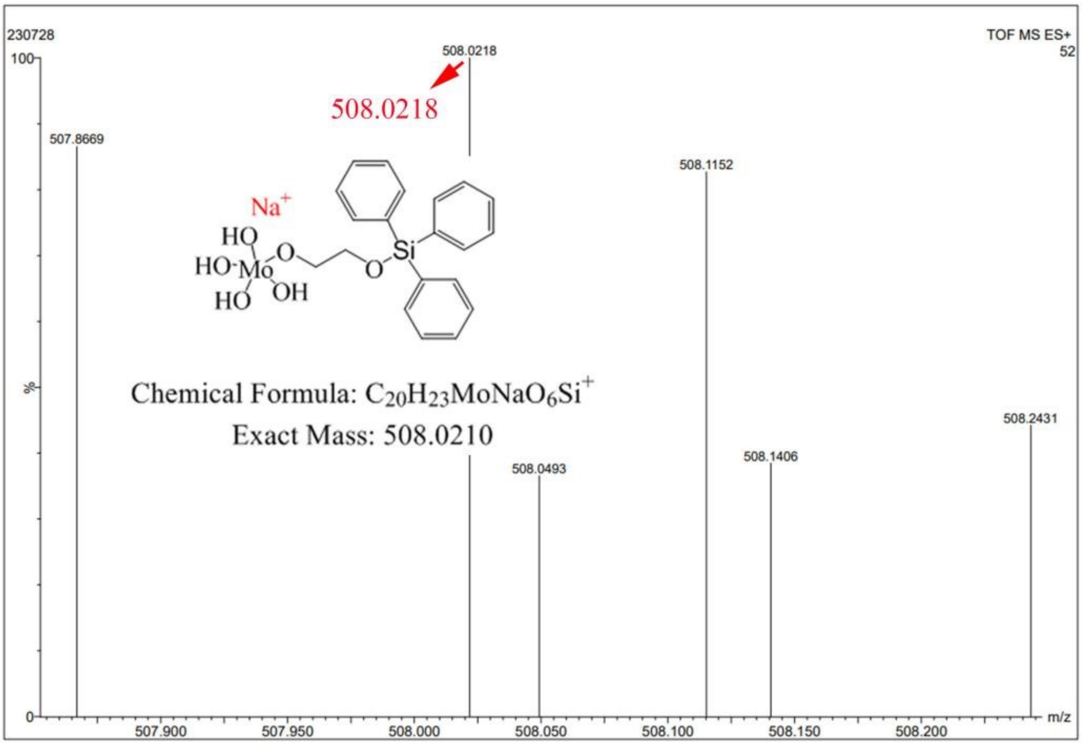

Fig. S2 Mass spectra of molybdenum pentachloride ($MoCl_5$) and triphenyl silyl chloride ($(C_6H_5)_3SiCl$) mixed with EG.

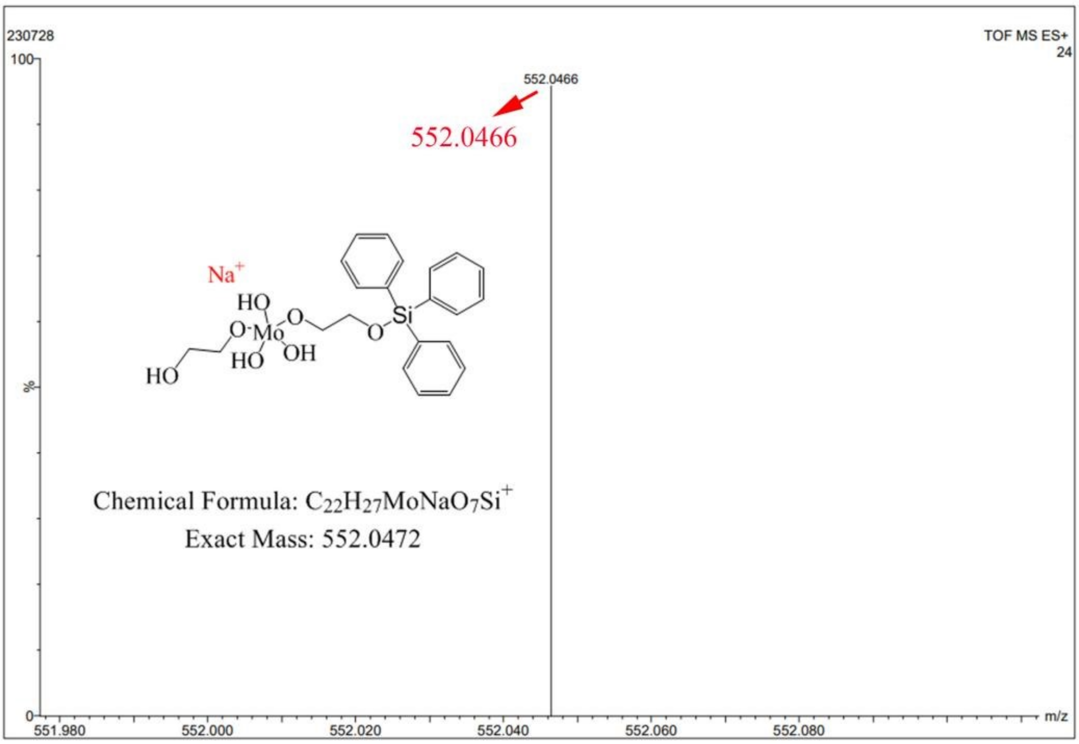

Fig. S3 Mass spectra of $MoCl_5$ and $(C_6H_5)_3SiCl$ mixed with EG.

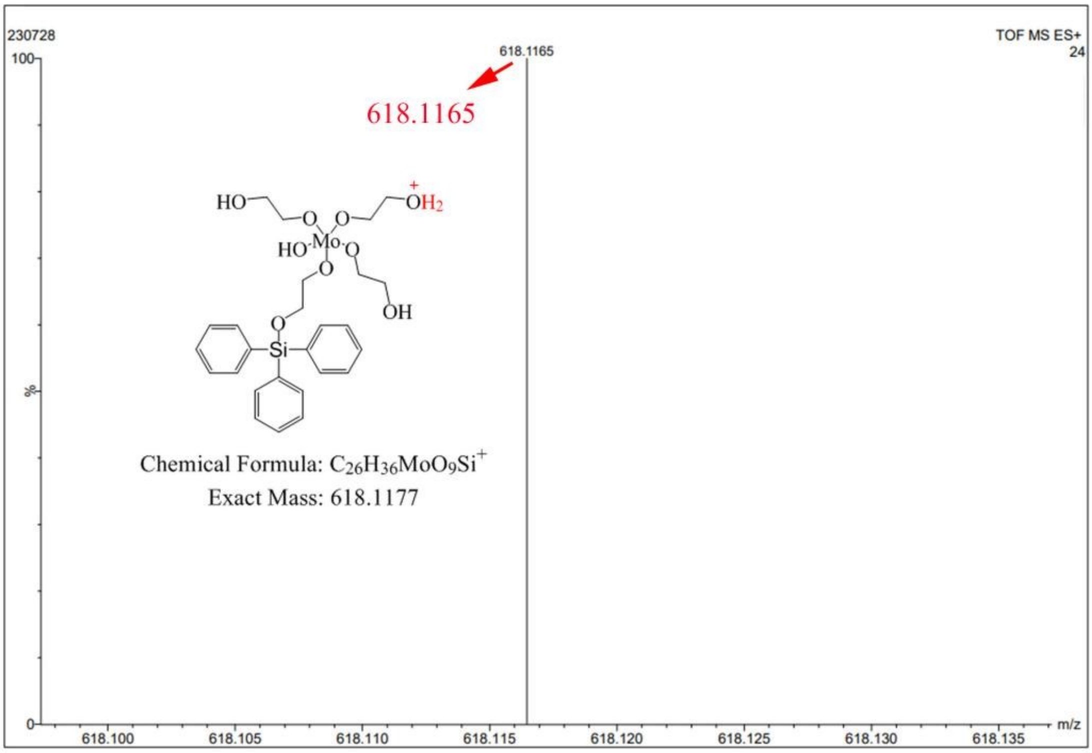

Fig. S4 Mass spectra of $MoCl_5$ and $(C_6H_5)_3SiCl$ mixed with EG.

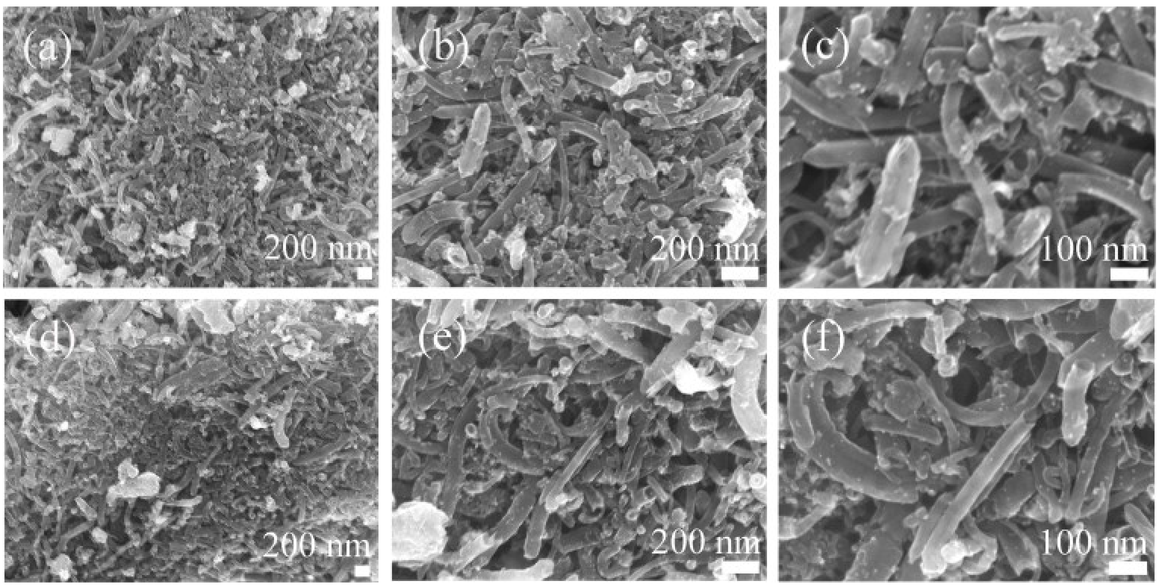

Fig. S5. Two sets of SEM images of C@SiO_x@NMWCNT (a-c) and (d-f).

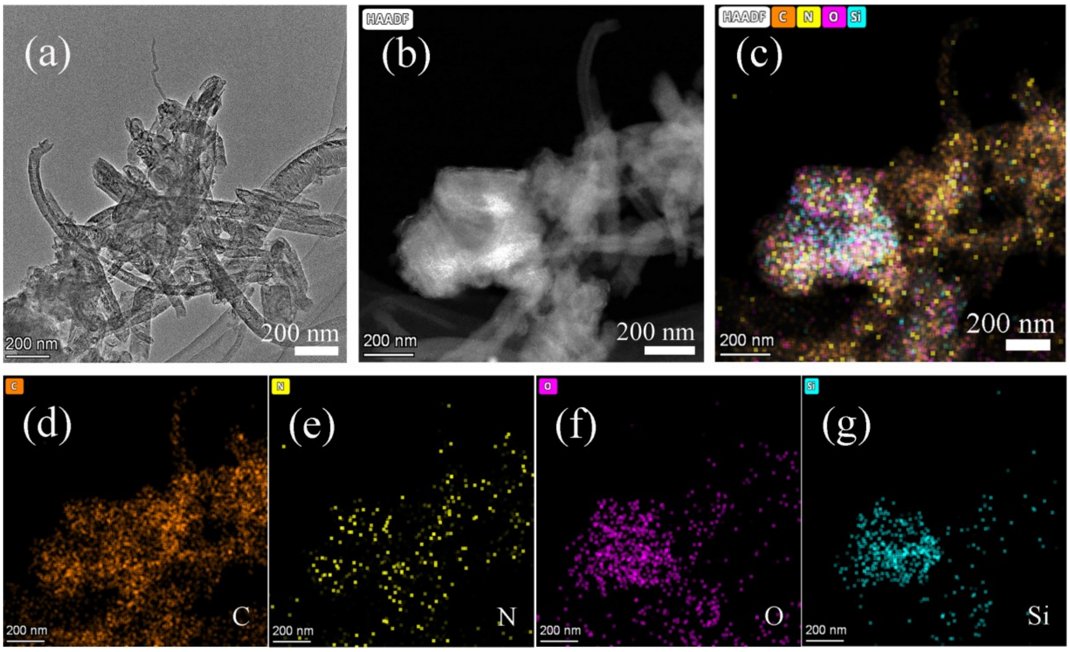

Fig. S6 (a) TEM images of C@SiO_x@NMWCNT, (b) STEM images of C@SiO_x@NMWCNT, (c) Elemental distribution of C@SiO_x@NMWCNT and corresponding (d), (e), (f) and (g) EDS-mapping element maps.

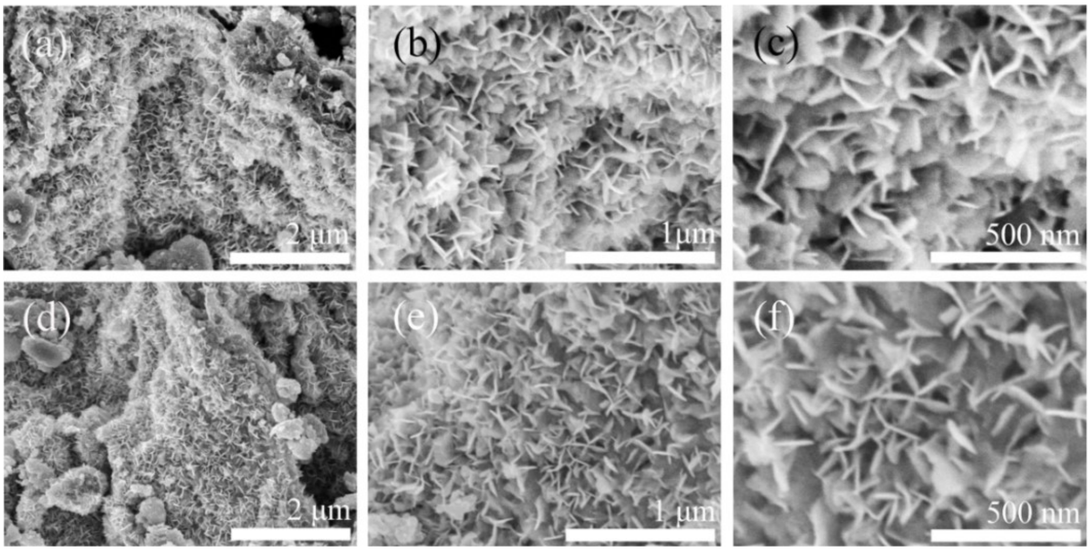

Fig. S7 Two sets of SEM images of C@SiO_x/$MoSe_2$@C (a-c) and (d-f).

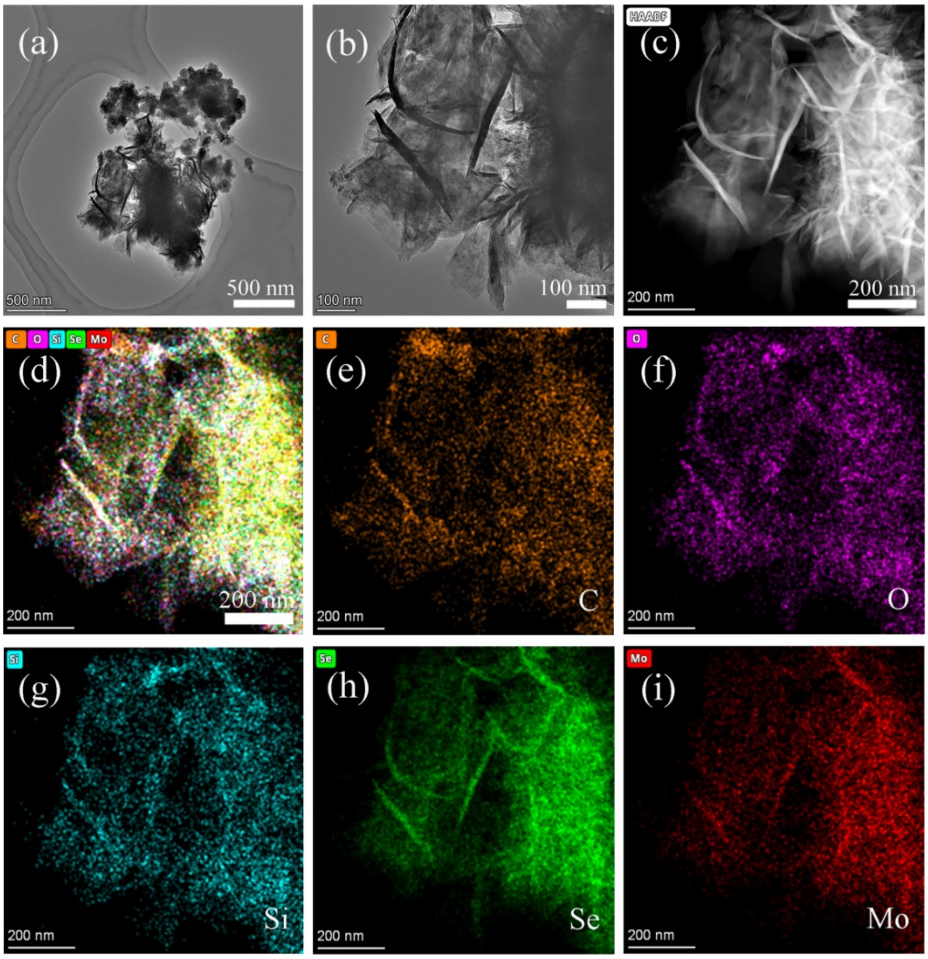

Fig. S8 (a-b) TEM images of C@SiO_x/$MoSe_2$@C, (c) STEM images of C@SiO_x/$MoSe_2$@C, (d) Elemental distribution of C@SiO_x/$MoSe_2$@C and corresponding (e), (f), (g), (h) and (i) EDS-mapping element maps.

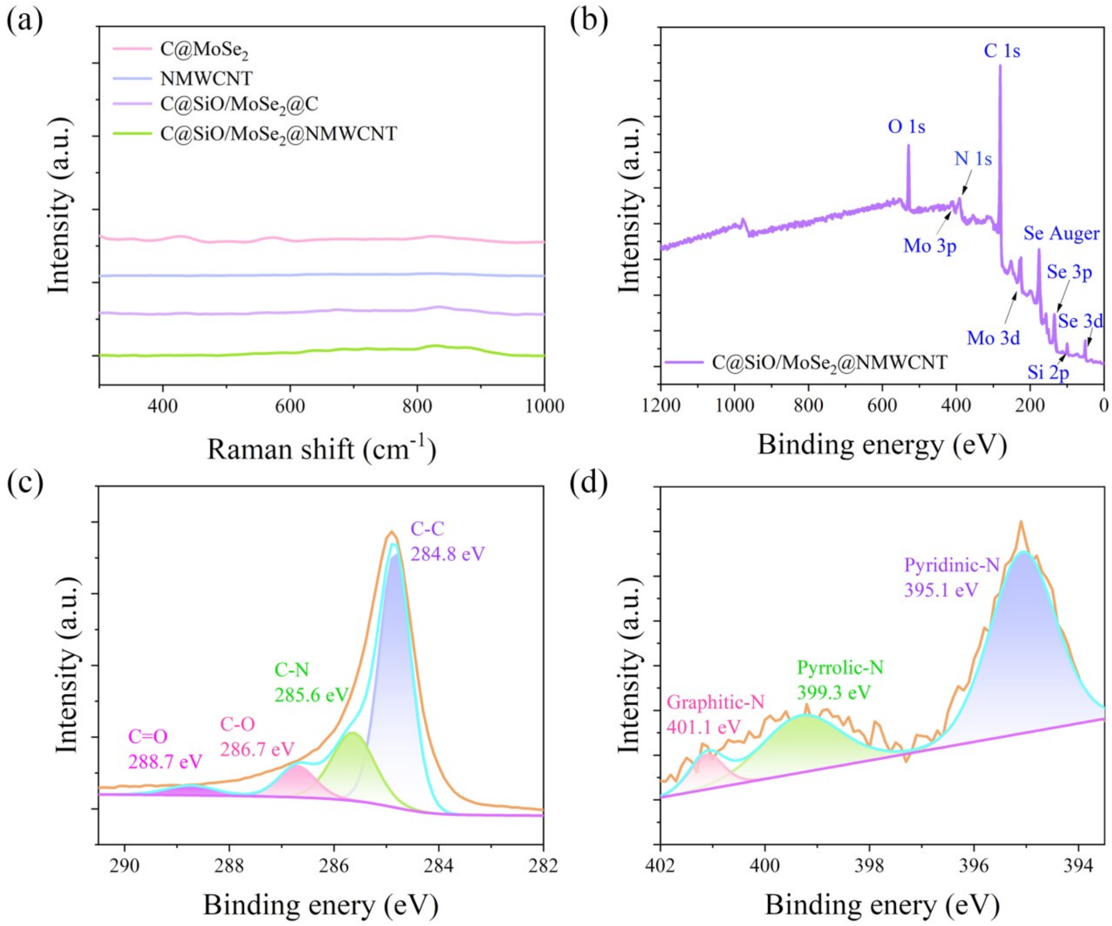

Fig. S9 (a) Raman shift of C@$MoSe_2$, NMWCNT, C@SiO_x/$MoSe_2$@C, C@SiO_x/$MoSe_2$-3:1@NMWCNT, (b) XPS full spectrum of C@SiO_x/$MoSe_2$-3:1@NMWCNT, the high-resolution XPS (c) C 1s spectrum, (d) N 1s spectrum.

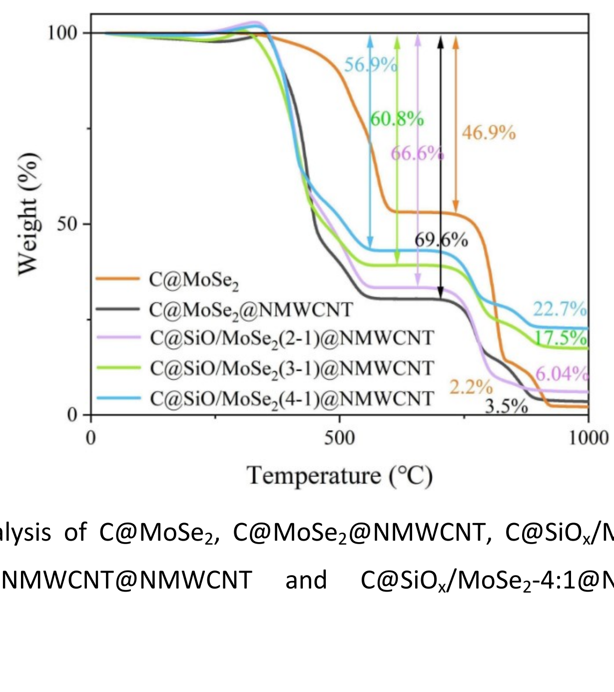

Fig. S10 The TG analysis of C@$MoSe_2$, C@$MoSe_2$@NMWCNT, C@SiO_x/$MoSe_2$-2:1@NMWCNT, C@SiO_x/$MoSe_2$-3:1@NMWCNT@NMWCNT and C@SiO_x/$MoSe_2$-4:1@NMWCNT composite systems.

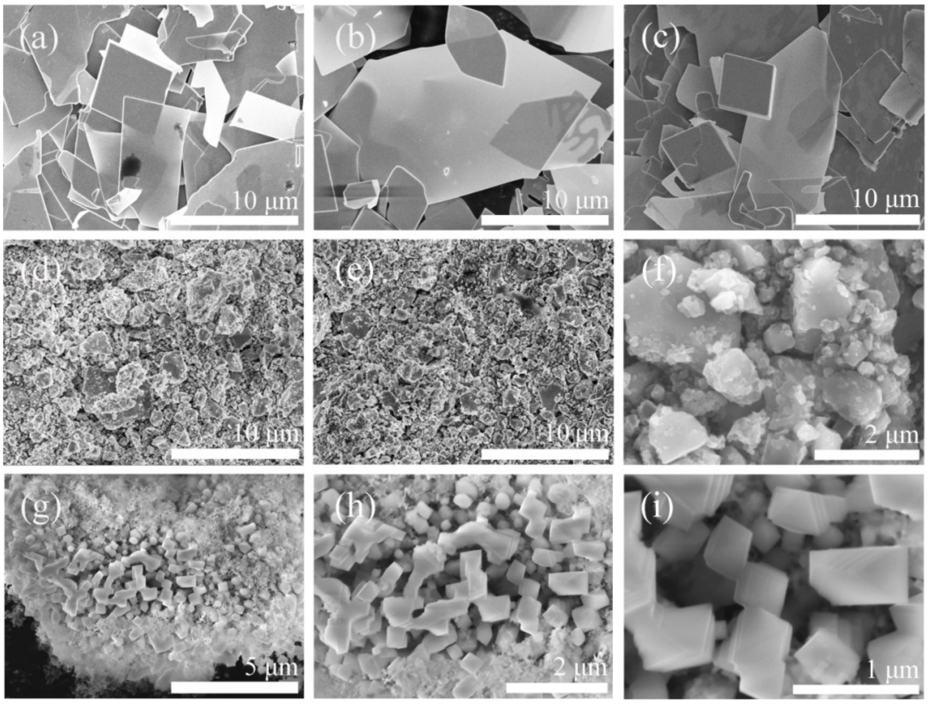

Fig. S11 SEM images of C@$MoSe_2$-Air (900℃) (a-c), C@$MoSe_2$@NMWCNT (900℃) (d-f), C@SiO_x/$MoSe_2$-3:1@NMWCNT-Air (900℃) (g-i), they represent residues obtained by calcination at 900℃ for four hours in an air environment.

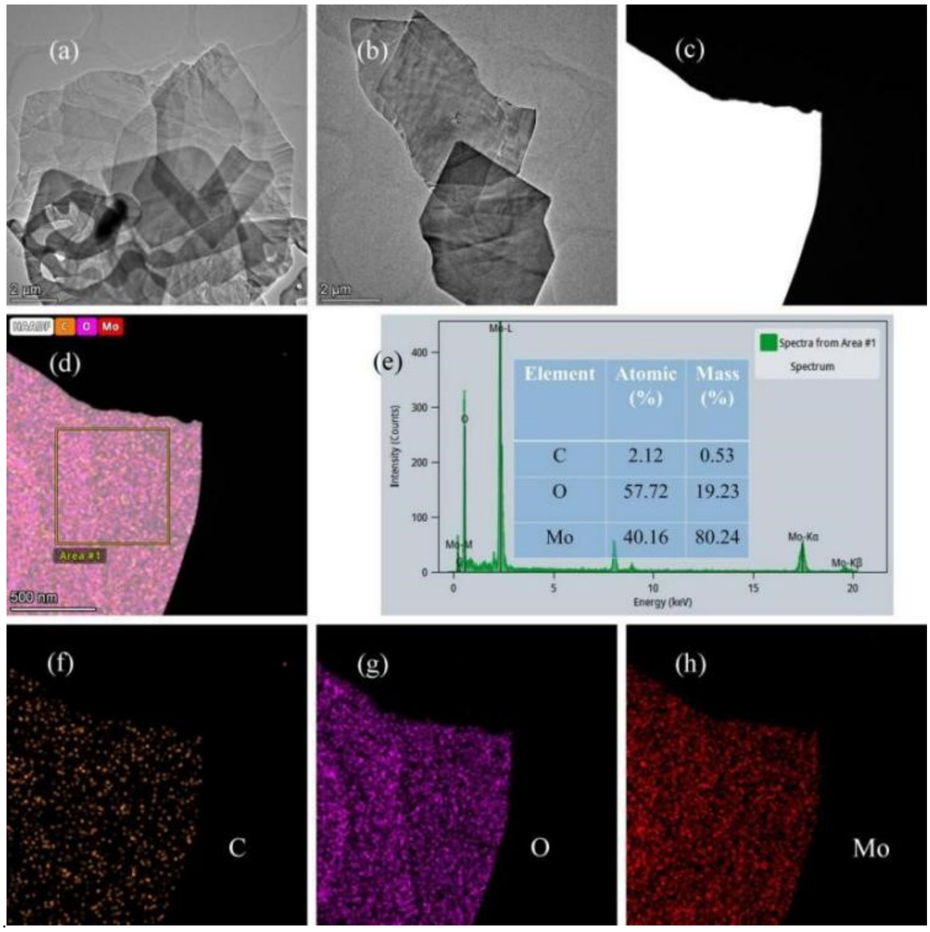

Fig. S12 (a-b) TEM images of C@$MoSe_2$-Air (900℃), (c) STEM images of C@$MoSe_2$-Air (900℃), (d) Eleental distribution of C@$MoSe_2$-Air (900℃) and corresponding (f), (g) and (h) EDS-mapping element maps.

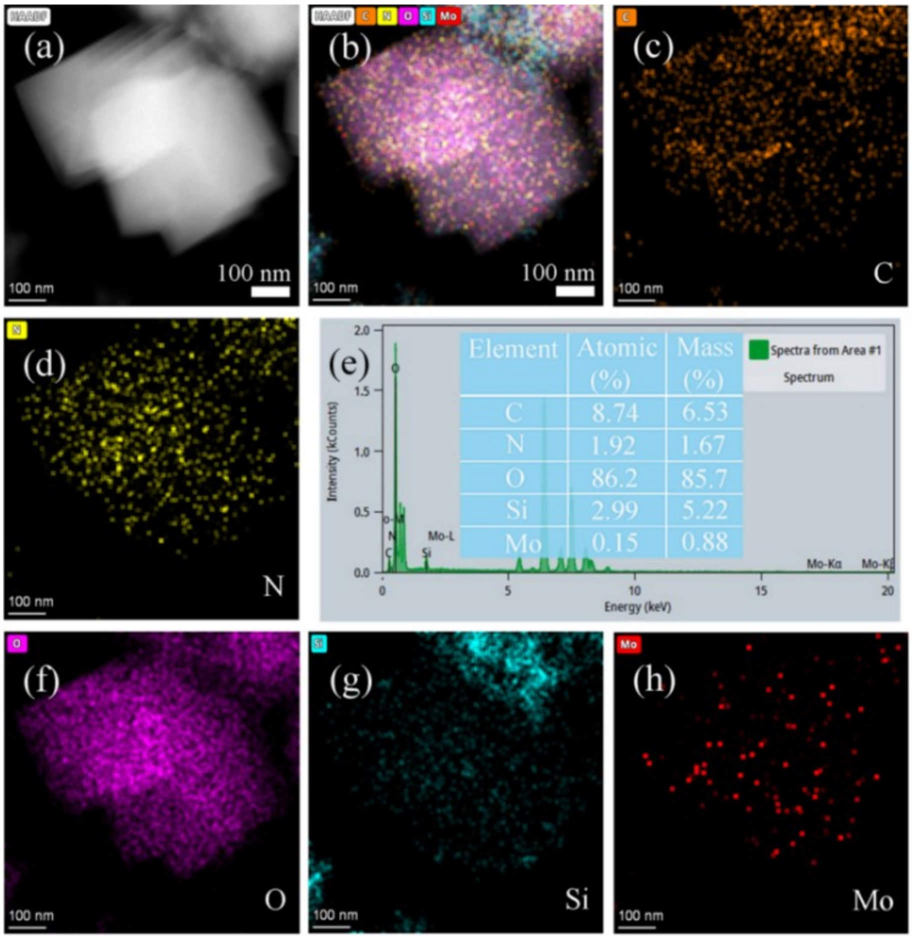

Fig. S13 (a) STEM image of C@SiO_x/$MoSe_2$-3:1@NMWCNT-Air (900℃), (b) Elemental distribution of C@SiO_x/$MoSe_2$-3:1@NMWCNT-Air (900℃) and corresponding (c), (d), (f), (g) and (h) EDS-mapping element maps.

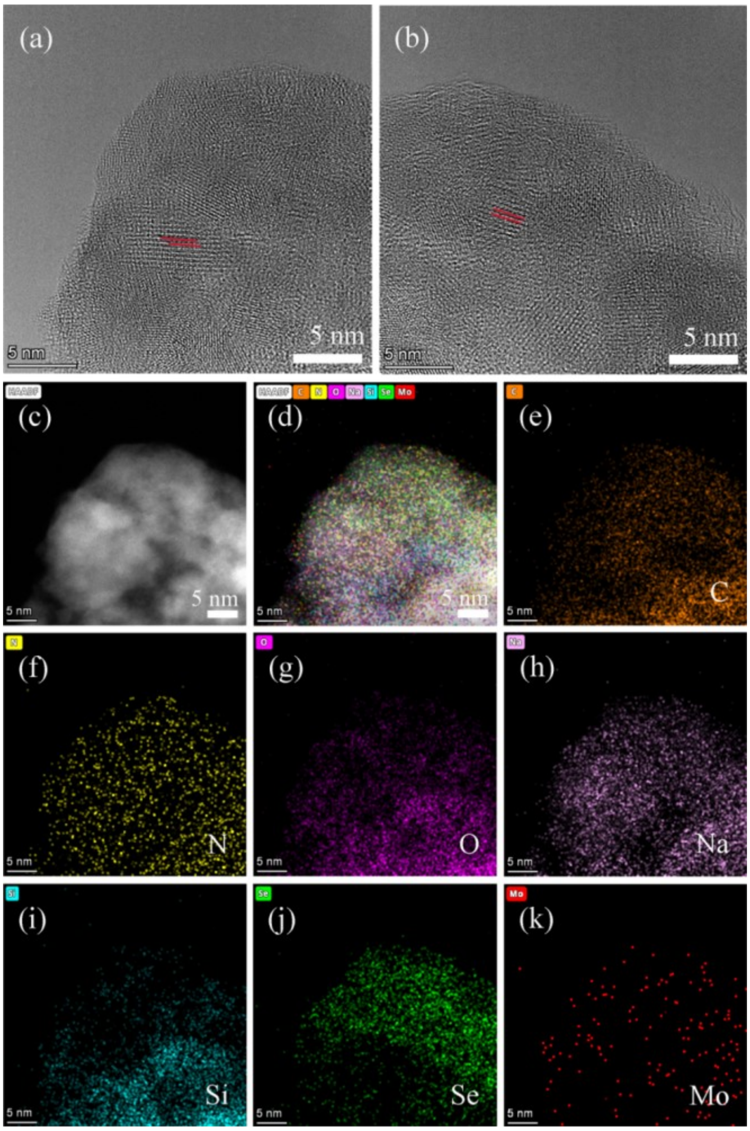

Fig. S14 (a-b) ex situ HRTEM image of C@SiOx/MoSe2-3:1@NMWCNT, (c) STEM image of C@SiOx/MoSe2-3:1@NMWCNT, (d) Elemental distribution of C@SiOx/MoSe2-3:1@NMWCNT and corresponding (e), (f), (g), (h), (i), (j) and (k) EDS-mapping element maps. (Charge from open circuit voltage 0.01 V to 3 V).

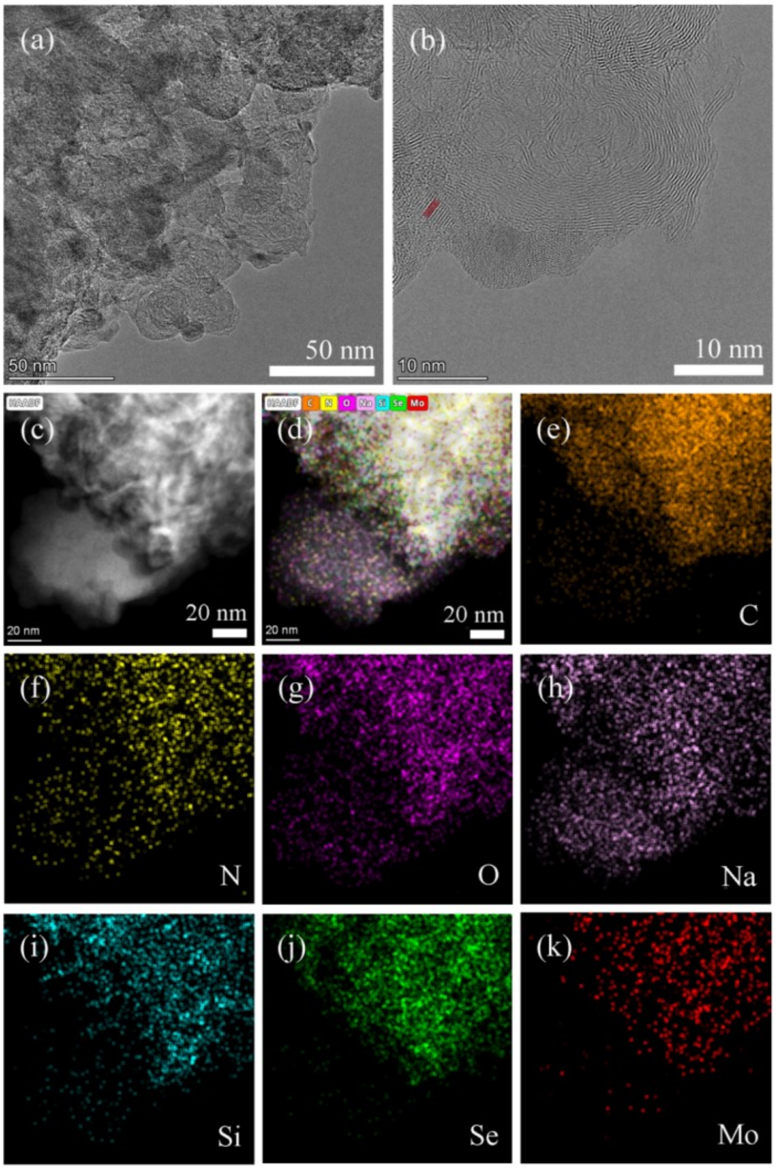

Fig. S15 (a) Non-in situ TEM image of C@SiO_x/$MoSe_2$-3:1@NMWCNT, (b) HRTEM image of C@SiO_x/$MoSe_2$-3:1@NMWCNT, (c) STEM image of C@SiO_x/$MoSe_2$-3:1@NMWCNT, (d) Elemental distribution of C@SiO_x/$MoSe_2$-3:1@NMWCNT and corresponding (e), (f), (g), (h), (i), (j) and (k) EDS-mapping element maps. (Charge from open circuit voltage 0.01 V to 2 V).

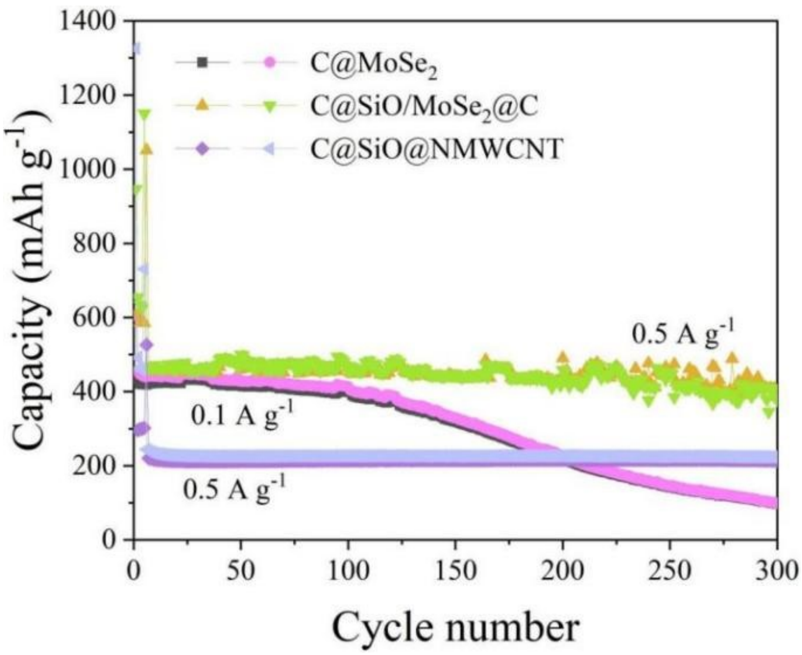

Fig. S16 The discharge/charge profiles (0.1 A g^{-1}) of C@$MoSe_2$ and the discharge/charge profiles (0.5 A g^{-1}) of C@SiO_x/$MoSe_2$@C, C@SiO_x@NMWCNT.